Journal of Cellular Biochemistry 91:1218–1238 (2004)

Promoter Activity and Regulation of the Corneal CYP4B1 Gene by Hypoxia

Vladimir Mastyugin, Alexandre Mezentsev, Wen-Xiang Zhang, Silvia Ashkar, Michael W. Dunn, and Michal Laniado-Schwartzman*

Department of Pharmacology, New York Medical College, Valhalla, New York

Abstract Hypoxic injury to the ocular surface provokes an inflammatory response that is mediated, in part, by corneal epithelial-derived 12-hydroxyeicosanoids. Recent studies indicate that a cytochrome P450 (CYP) monooxygenase, identified as CYP4B1, is involved in the production of these eicosanoids which exhibit potent inflammatory and angiogenic properties. We have isolated and cloned a corneal epithelial CYP4B1 full-length cDNA and demonstrated that the CYP4B1 mRNA is induced by hypoxia in vitro and in vivo. To further understand the molecular regulation that underlies the synthesis of these potent inflammatory eicosanoids in response to hypoxic injury, we isolated and cloned the CYP4B1 promoter region. GenomeWalker libraries constructed from rabbit corneal epithelial genomic DNA were used as templates for primary and nested PCR amplifications with gene- and adaptor-specific primers. A 3.41-kb DNA fragment of the 5′-flanking region of the CYP4B1 promoter was isolated, cloned, sequenced, and analyzed by computer software for the presence of known *cis*-acting elements. Analysis of the promoter sequence revealed the presence of consensus DNA binding sequences for factors known to activate gene transcription in response to hypoxia including HIF-1, NFκB, and AP-1. Transient transfection of luciferase reporter (pGL3-Basic) vectors containing different lengths of the CYP4B1 promoter fragment demonstrated hypoxia-induced transcription in rabbit corneal epithelial (RCE) cells. Electrophoretic mobility shift assay (EMSA) revealed a marked induction of nuclear binding activity for the labeled HIF-1 probe from the CYP4B1 promoter in nuclear extracts of cells exposed to hypoxia. This binding activity was due to sequence-specific binding to the HIF-1 oligonucleotide probe as shown by competition with excess unlabeled probe for the HIF-1 but not with unlabeled NFκB probe. The nuclear binding activity of AP-1 and NFκB probes from the CYP4B1 promoter was also enhanced in response to hypoxia suggesting that these transcription factors contribute to the hypoxic induction of CYP4B1 expression. The results of this study provide the first molecular mechanistic explanation for the induction of CYP4B1 and, thereby, the production of inflammatory eicosanoids in response to hypoxic injury. Further studies are needed to fully evaluate the molecular regulation of this gene during inflammation. J. Cell. Biochem. 91: 1218–1238, 2004.

Key words: Hypoxia inducible factor-1; Eicosanoids; Inflammation; NFκB; AP-1

Injury to the cornea provokes an inflammatory response with the degree of inflammation correlating to the severity of the injury. Numerous mediators are involved in the development and progression of corneal inflammation, among them are the arachidonic acid-derived eicosanoids produced by the cyclooxygenases, lipoxygenases, and cytochrome P450 (CYP) monooxygenases, i.e., prostaglandins, leukotrienes, and HETEs, which have been implicated in the initiation, development, and progression of an inflammatory response. Studies in our laboratory have identified CYP-dependent arachidonic acid metabolism in the corneal epithelium and established it as a primary inflammatory pathway in rabbit models of ocular surface inflammation. Corneal epithelial CYP metabolizes arachidonic acid to 12(*R*)-hydroxy-5,8,10,14-eicosatetraenoic acid [12(*R*)-HETE], a potent Na,K-ATPase inhibitor and 12(*R*)-hydroxy-5,8,14-eicosatrienoic acid [12(*R*)-HETrE], a vasodilator, chemotactic, and angiogenic factor [Laniado Schwartzman, 1997].

Grant sponsor: National Eye Institute; Grant number: EY06513.

*Correspondence to: Michal Laniado-Schwartzman, PhD, Department of Pharmacology, New York Medical College, Valhalla, NY 10595.

E-mail: michal_schwartzman@nymc.edu

Received 22 September 2003; Accepted 14 November 2003

DOI 10.1002/jcb.20018

Several lines of evidence provide strong support for the involvement of the CYP-derived metabolites, in particular 12(*R*)-HETrE, in the inflammatory response: (1) Following hypoxic or chemical injury to the surface of the cornea, the corneal epithelial capacity to synthesize 12-HETE and 12-HETrE is greatly enhanced and significantly correlated with the appearance and course of the inflammatory response, thereby, indicating a potential cause–effect relationship between these events [Conners et al., 1995a, 1997]; (2) depletion of CYP proteins inhibited 12-HETE and 12-HETrE synthesis and markedly attenuated the inflammatory response to hypoxic injury, further providing strong pharmacological evidence for the role of CYP-derived arachidonic acid metabolites in these models of ocular surface inflammation [Conners et al., 1995b; Laniado Schwartzman, 1997]. (3) Human corneal epithelium exhibits CYP-dependent arachidonic acid metabolism and 12-HETE and 12-HETrE are present in normal open eye human tears in very low concentrations. Moreover, the level of the proinflammatory angiogenic metabolite, 12-HETrE, is several fold higher in tears from subjects with ocular surface inflammation, further supporting a role for these eicosanoids in human ocular pathophysiology [Mieyal et al., 2001].

Recent studies led to the isolation of a 0.67-kb corneal epithelial cDNA with a 98.8% sequence homology to the rabbit lung CYP4B1 isoform [Mastyugin et al., 1999]. Its expression in corneal organ cultures was induced by hypoxia and by chemical inducers of the CYP4 gene family such as clofibrate and phenobarbital; its increased expression was associated with increased production of 12-HETE/12-HETrE [Mastyugin et al., 1999]. Further studies demonstrating that antibodies against CYP4B1 inhibited hypoxia-induced 12-HETE and 12-HETrE synthesis [Mastyugin et al., 1999] provided substantial evidence that in the corneal epithelium CYP4B1 is involved in hypoxia-induced 12-HETE and 12-HETrE synthesis and ocular surface inflammation. Indeed, in a recent study we documented the increased expression of CYP4B1 mRNA in the corneal epithelium during hypoxic injury in vivo. The pattern of expression of CYP4B1 corresponded well with the progression of the anterior surface inflammatory response including corneal thickness and inflammatory score as well as with the rate of synthesis of the inflammatory and angiogenic eicosanoid 12-HETrE [Mastyugin et al., 2001].

To start elucidating the molecular mechanisms responsible for the regulation of this gene, particularly in response to hypoxia, studies were carried out to isolate, clone, and analyze the corneal epithelial CYP4B1 full-length cDNA and its promoter region. The findings of sequences on the promoter region of the corneal *CYP4B1* gene that are recognized by transcription factors whose activity is regulated by hypoxia provides a molecular mechanistic explanation for the induction of CYP4B1 and, thus, the production of inflammatory eicosanoids in response to hypoxic injury.

MATERIALS AND METHODS

Materials

Rabbit eyes from 8–12-week-old male and female New Zealand White or California White rabbits (1.6–2.5 kg) were obtained from Pel-Freez Biologicals (Rogers, AK). All chemicals were molecular biology grade and purchased from Sigma (St. Louis, MO). Cell culture reagents were obtained from Invitrogen (Carlsbad, CA). Restriction endonucleases were purchased from New England Biolabs, Inc. (Beverly, MA). pBluescript II KS+ was obtained from Stratagene (La Jolla, CA). The pGL3-Basic firefly luciferase receptor vector pGL3-B was obtained from Promega (Carlsbad, CA). Oligonucleotide primers were synthesized by Gene Link, Inc. (Thornwood, NY).

Corneal Organ Culture

Fresh eyes were shipped overnight on ice in Hanks balanced salt solution (HBSS) containing 100 μg/ml penicillin G, 100-U/ml streptomycin sulfate, and 0.25 μg/ml amphotericin B (Fungizone, Invitrogen, Carlsbad, CA). Eyes were washed in Dulbecco's modified eagles medium (DMEM) with 2× penicillin/streptomycin/Amphotericin B; corneas were dissected with the scleral rim intact. The corneas were washed five times with the same medium and each cornea was transferred to a well in a 12-well plate containing 1 ml of DMEM with 0.2% lactalbumin enzymatic hydrolysate (LH) and 1× penicillin/streptomycin/Amphotericin. Culture plates were placed in a 37°C incubator supplied with 5% CO_2/95% air (normoxia); or in a modular tissue culture chamber (Billups-Rothenburg, DelMar, CA) supplied continuously

with 5% CO_2/2% O_2/93% N_2 (hypoxia), bubbled through deionized H_2O into the chamber within a 37°C incubator. Cultures were incubated for 2–24 h without change of medium.

Cloning of CYP4B1 Full-Length cDNA

Gene-specific primers (GSPs) were designed based on the defined sequence of the hypoxia-induced corneal CYP4B1 0.67-kb cDNA fragment [Mastyugin et al., 1999] (GenBank accession no.: AF176914) and are listed in Table I. Isolated rabbit corneas were placed under hypoxic conditions as described above. Two hours later, corneal epithelium was scraped and total RNA was extracted using TRIzol reagent (Invitrogen). The first strand cDNA synthesis reaction was catalyzed by SuperScript™ II RNase H^- reverse transcriptase (RT), supplied by 3′- and 5′-RACE kits (Invitrogen). Amplification of RACE products was carried out in a final volume of 100 μl consisting of 20 mM Tris-HCl (pH 8.8), 10 mM potassium chloride, 10 mM ammonium sulfate, 2.0 mM magnesium sulfate, 1% Triton X-100, 1 mg/ml nuclease-free bovine serum albumin, 200 μM of each deoxyribonucleoside triphosphate, 5 μl of the DNA template (first-strand cDNA product or diluted 1:100 first round PCR mix), 0.2 μM of each forward and reverse primer, and 2.5 U of the PfuTurbo DNA polymerase (Stratagene, La Jolla, CA). The reactions were heated to 97°C for 1 min and cycled 30 times through a 1 min denaturing step at 97°C, a 1.5 min annealing step at 55°C, and a 2.0-min extension step at 72°C. After the cycling procedure, a final 10-min elongation step at 72°C was performed.

3′-RACE and 5′-RACE products were digested using one of the restriction endonuclease sites designed into the AUAP (*Not I* site). We also designed a unique restriction site (*Acc I*) within the gene-specific primers. The RACE product was treated with T4 DNA polymerase in the presence of dATP and dTTP to create defined cohesive ends. The resulting RACE product was ligated into a nondephospharylated *Not I–Acc I*-cut pBluescript II KS+ vector (Stratagene) using T4 DNA ligase. *MAX Efficiency DH5α Cells* (Invitrogen) were then transformed with the vector-ligated DNA. Positive clones were amplified and plasmid DNA purified using a QIAprep Miniprep Kit (Qiagen, Valencia, CA). Plasmid DNA was analyzed by PCR with standard pBluescript II KS+ primers RP and T7 to assess insert size. PCR products were resolved on 1.2% agarose gels stained with ethidium bromide, visualized under UV light, and the image was captured on Polaroid film.

The primary structure of the RACE products was established by sequencing using the dye terminator cycle sequencing method with standard pBluescript II KS+ T3 and T7 primers. Primary RACE products were also directly sequenced with gene-specific primers, GSP-1F and GSP-2. Nucleotide sequencing was performed by Davis Sequencing (San Diego, CA). Primary RACE products were also directly

TABLE I. Primer Sequences

Name	Sequence, 5′-
3′-RACE adapter primer (3AP)	GGCCACGCGTCGACTAGTACTTTTTTTTTTTTTTTT
3′-RACE abridged universal amplification primer (3AUAP), homologous to the adapter sequence	GGCCACGCGTCGACTAGTACTT
3′-RACE gene-specific primer (GSP-2F)	CGATTCTCTTGGATGTCCGCGGT
3′-RACE nested primer (GSP-1F)	CGATTTCCTCTACTGCATGGCCTT
5′-RACE abridged anchor primer (5AAP)	GGCCACGCGTCGACTAGTACGIIGGGIIGGGIIG
5′-RACE abridged universal amplification primer (5AUAP), homologous to the adapter sequence	GGCCACGCGTCGACTAGTAC
5′-RACE gene-specific primer GSP-1, anneals to mRNA	TGTCTCCTTTGCCAAACGTACAC
5′-RACE gene-specific primer GSP-2, amplification of the dC-tailed cDNA using the 5AUAP	CGATGTGGCCCACGTCAGAGAAG
5′-RACE nested gene-specific primer GSP-3 (re-amplification of the primary PCR product)	CGATGTCGAAGCTCTTACCCTCAC
Standard pBluescript II KS+ primer RP	GGAAACAGCTATGACCATGATT
Standard pBluescript II KS+ primer T7	GTAATACGACTCACTATAGGGC
Standard pBluescript II KS+ primer T3	ATTAACCCTCACTAAAGGGA
Gene-specific primer 4B1-FP	CCTCTCCTGAGCGTCGCTGTCT
Gene-specific primer 4B1-RP	GTGAGTTCTGTTTATTCAGCATCGTG
Adapter-specific 5′-primer (AS5P)	GTAATACGACTCACTATAGGGC
Gene-specific 3′-primer-1 (GS3P1)	(CAACCTCTGCCTTCGAAGCAGCAGGCGGAGGA)
Nested 5′-primer (N5P1)	ACTATAGGGCACGCGTGGT
Nested 3′-primer (N3P1)	GAGGAAGCCTAGGATCAAGATCAGTCCGGAAGCC
Gene-specific 3′-primer-2 (GS3P2)	ACCCATTTAACCGGGACAACAGGAGAT
Nested 3′-primers (N3P2)	GCCAGCCTCATGAAGTTCTGATTCCTT

sequenced with the gene-specific primers, 4B1-FP and 4B1-RP. Nucleotide sequences corresponding to the RACE product were aligned to all available GenBank sequences and compared against the known sequence of rabbit lung CYP4B1.

Isolation of the Rabbit CYP4B1 Promoter Region

Rabbit corneal genomic DNA was extracted using the DNeasy Tissue Kit (Qiagen, Valencia, CA). The GenomeWalker kit (Clontech, Palo Alto, CA) was used for the isolation of the 5′-flanking region of the rabbit *CYP4B1* gene. Briefly, samples of rabbit cornea genomic DNA were separately digested with five different restriction enzymes. Digested DNA fragments were then adapter-ligated to produce five sets of DNA fragments with adapters at their ends. Each set of DNA fragments was amplified using an adapter-specific 5′-primer and a rabbit *CYP4B1* gene-specific 3′-primer, GS3P1. The second PCR reaction was done using nested primers, N5P1 and N3P1. The PCR products from each set were analyzed on a 1.2% agarose gel. Two different sets showed major PCR products corresponding to 1.8 and 0.65 kb, respectively. These products were digested with *Sal I* (incorporated within the nested 5′-primer) and cloned into the pBluescript II KS+ vector digested with *Sal I* and *Sma I*. Nucleotide sequences were determined by the dye terminator cycle sequencing method (Davis Sequencing). Based on the sequencing data, the primers GS3P2 and N3P2 were designed for further genomic walking using the same GenomeWalker kit. For Southern blot analysis, rabbit genomic DNA was digested with either *Eco*RV, *Dra*I, *Pvu*II, or *Hind*III, fractionated on a 0.7% agarose gel, transferred to Hybond-N^+, and hybridized with a ^{32}P-labeled fragment (−2535 to −1755) of the isolated CYP4B1 promoter.

Construction of Luciferase Reporter Plasmids

The Luciferase reporter constructs containing various deletions of the CYP4B1 promoter were prepared by direct cloning of PCR products and subsequent deletion using restriction enzyme digestion. The pGL3-Basic firefly luciferase receptor vector (pGL3-B) (Promega), which does not have any promoter and enhancer elements, served as a negative control. The deletion constructs (−3435/+22, −1787/+22, −955/+22, −640/+22, −194/+22) were subcloned upstream of the firefly luciferase reporter gene of pGL3-B employing *Kpn*I and *Hind*III sites. The 3′-end of each luciferase reporter construct is located +22 relative to the CYP4B1 transcriptional start site, whereas the 5′-ends map to various position of the promoter as indicated above. All constructs were sequenced and/or restriction enzyme digested to confirm their authenticity.

Cell Transfection and Luciferase Assay

The rabbit corneal epithelial cell line was obtained from Dr. Kaoru Araki-Sasake, Osaka University [Araki et al., 1993]. RCE cells were grown in medium containing a mixture of DMEM/F12 1:1, 10% FBS, and 1% antibiotic/antimycotic mixture. For transfection, cells were seeded at 2×10^5 cells/well in 12-well plates and grown to 80% confluency at 37°C in a 5% CO_2 incubator. Cells were washed with PBS and 0.8 ml of Opti-MEM (Invitrogen) was added into each well together with a mixture containing 0.3 μg of either empty vector (pGL3-B) or promoter deletion constructs and 1.5 μl of LipofectAMINE 2000 (Invitrogen) in 0.2 ml of Opti-MEM. Renilla luciferase reporter vector phRL-TK (25 ng) was co-transfected in all experiments as an internal standard for transfection efficiency. Five hours after transfection, medium was replaced with 1 ml of DMEM containing 0.1% FBS and cells were incubated overnight at 37°C in a 5% CO_2 incubator. Twenty-four hours later, cells were placed under normoxia (5% CO_2, balanced with air) or hypoxia (2% O_2, balanced with 5% CO_2, 95% N_2) for additional 24 h. In some experiments, transfected cells were incubated in the presence of 3-MC (2 μM) under normoxia or hypoxia for additional 24 h as previously described [Mastyugin et al., 1999]. Control cells were transfected in parallel and cultivated under normal oxygen tension. A dual luciferase reporter assay system (Promega) and a luminometer (Turner Designs, Sunnyvale, CA) were used for luciferase activity assay. Cells were lysed and assayed for luciferase activity according to manufacturer's protocol.

Electrophoretic Mobility Shift Assay (EMSA)

Nuclear extracts of RCE cells exposed to normoxia and hypoxia for 1 or 4 h were prepared as previously described [Laniado-Schwartzman et al., 1994]. EMSA was performed with ^{32}P-

labeled double stranded oligonucleotides containing consensus DNA binding sequences within the CYP4B1 promoter for the following transcription factors: HIF-1 (−871 to −852; 5′-aggaaaCACGTGgggtgaat-3′ and −78 to −64; gcaggGCGTGgcgag), NFκB (−1136 to −1112; 5′-ggaTGGGAGACTCCagcaagagatt-3′) and AP-1 (−1290 to −1272; 5′-atgtctgTGAGTCAgcacc-3′). Oligonucleotides were labeled using [γ-^{32}P]ATP and T4 polynucleotide kinase or [α-^{32}P]dCTP and Klenow large fragment of DNA polymerase I according to manufacturer protocols (Invitrogen). Labeled oligonucleotides were purified with QIAquick Nucleotide Removal Kit (Qiagen). Nuclear extracts (10 μg) were preincubated in 20 μl reaction mixtures containing 10 mM Tris-HCl, pH 7.5, 1 mM EDTA, 1 mM dithiothreitol, 10% glycerol, and 1 μg of salmon testis DNA (Sigma-Aldrich, St. Louis, MO) at room temperature for 5 min. ^{32}P-labeled double stranded oligonucleotide probe (10,000 cpm) was added, and the incubation was continued for another 20 min. For oligonucleotide competition, unlabeled oligonucleotide probe (100-fold molar excess) was added during the preincubation period. Reaction products were then fractionated on a 5% polyacrylamide gel in 1× Tris-Gly-EDTA buffer, pH 8.3 at 70 V for 30 min followed by 3 h at 170 V. Gels were dried, autoradiographed, and quantified by densitometry analysis. Supershift assays were performed using the following antibodies (Santa Cruz Biotechnology, Inc., Santa Cruz, CA): rabbit anti c-fos (H-206) polyclonal antibody, goat anti HIF-1α (C-19) polyclonal antibody, goat anti NFκB p50 (C-19) polyclonal antibody, and rabbit anti NFκB p65 (A) polyclonal antibody.

RESULTS

Isolation, Cloning, and Sequencing of Full-Length cDNA

The reconstructed sequence of the rabbit corneal cDNA is shown in Figure 1. Two slightly dissimilar sequences were obtained from different batches of rabbit corneal epithelium. The first sequence was identical to the lung CYP4B1 isoform (GenBank accession no.: M29852), while the second sequence was slightly different from the lung isoform (Fig. 1). Thus, substitution of G (Lung) with A (Cornea) yields *isoleucine* instead of *valine* and substitution of C (Lung) with A (Cornea) yields *methionine* instead of *leucine*. These changes are for similar hydrophobic amino acids and may or may not confer functional differences.

The 5′-RACE product had an overlapping nucleotide sequence with the previously defined rabbit corneal CYP4B1 cDNA fragment (Fig. 1). Computer alignment of the 5′-RACE product to all available GenBank database sequences showed a high degree of sequence homology to the rabbit lung CYP4B1. Assuming the same position of the open reading frame for the corneal CYP4B1 as for the lung CYP4B1 isoform [Gasser and Philpot, 1989], the nucleotide sequences corresponding to the amplified portion of the coding region of the lung and corneal isoforms were identical. However, the 5′-untranslated region of the corneal CYP4B1 cDNA demonstrated some sequence differences as compared to the lung isoform. Corneal CYP4B1 cDNA was nine nucleotides longer in size and there were two mismatches: T_{10}, corneal CYP4B1-G_1, lung CYP4B1; C_{11}, corneal CYP4B1-G_2, lung CYP4B1. The observed differences in the nucleotide sequence may reflect the two different approaches used to clone and sequence the 5′-end region of the lung and the corneal CYP4B1 cDNA. Alternatively, the primary structures of the CYP4B1 transcripts in the lung and in the cornea may be different and tissue-specific. Thus, in the corneal epithelium, RNA polymerase II may utilize a different transcription initiation site, resulting in a longer 5′-untranslated region, which occurs in the corneal transcript.

The 3′-RACE product (Fig. 1) had the overlapping nucleotide sequence with the previously defined rabbit corneal CYP4B1 cDNA sequence. Computer alignment of the 3′-RACE sequence to all available GenBank database sequences showed a high degree of sequence homology to the rabbit lung CYP4B1. There was one mismatch in the region close to the putative heme-binding domain of the CYP (T_{1440}, 3′-RACE product, C_{1431}, rabbit lung CYP4B1). Based on the position of the open reading frame in the rabbit lung *CYP4B1* gene [Gasser and Philpot, 1989], this mismatch did not confer an amino acid change (*Phe* (F) to *Phe* (F)), implying no alterations in protein structure and function. The nucleotide sequence 5′-*CCTGAGGTCT-TTGACCCCCTGCGC* encoded the meander region polypeptide sequence PEVFD^{422}PLR, critical for heme binding to CYP4B1 [Zheng et al., 1998]. Assuming the same position of the

open reading frame for the corneal CYP4B1, the *stop* codon TAG was identical for lung and corneal isoforms. The nucleotide sequence 5′-*TTCTCTGCCGGGCCCAGGAACTGCATCGGGCAGCAGTTC* encodes the putative heme-binding region FSAGPRNCIGQQF. The presence of these conserved regions crucial for heme binding suggests that the corneal CYP4B1 isozyme is competent for heme binding, a key requirement of any functional P-450 enzyme.

The 3′-untranslated region was shorter than that of the lung CYP4B1, according to the position of the *stop* codon in the rabbit lung CYP4B1 isoform [Gasser and Philpot, 1989]. The poly-(A) signal followed immediately after the last nucleotide of the 3′-RACE product. This was confirmed by sequencing both the cloned 3′-RACE product with the standard vector-specific primers and the primary RACE product with the gene-specific primer. Occasionally, truncated cDNA 3′-ends are produced because of annealing of the modified oligo-(dT) primer to an A-rich region in the transcript upstream of the poly-(A). Alternatively, this poly-(A) signal could be a poly-(A) tail of the corneal CYP4B1 transcript that is not present in the rabbit lung CYP4B1 mRNA [Gasser and Philpot, 1989]. To further explore this possibility, a RT-PCR experiment was performed with the gene-specific primer used in the 3′-RACE (forward primer) and the primer derived from the 3′-terminal cDNA sequence of the rabbit lung CYP4B1 (reverse primer); the amplified PCR product exhibited the predicted size and the nucleotide sequence identical to the rabbit lung CYP4B1 (Fig. 1, long form). No "internal" poly-(A) sequence was detected. These results suggest that there might be several mRNA forms present in the rabbit corneal epithelium. The "truncated" corneal CYP4B1 transcript has a shortened non-coding region, which could have an important regulatory function. The presence of multiple transcripts may reflect a complicated mechanism responsible for the differential regulation of the CYP4B1 gene in the corneal epithelium in response to hypoxia and chemical injury.

The nucleotide sequences of two identified *corneal CYP4B1* transcripts were submitted to the GenBank database. A shorter transcript was determined as a "short form" and assigned the accession number AF176914. The longer transcript was introduced as a "long form" of the rabbit corneal CYP4B1 and assigned the accession number AF332576. Both forms showed 98–99% sequence identity with the rabbit lung CYP4B1 cDNA [Gasser and Philpot, 1989] and 72–77% sequence identity with the rat, human, and mouse CYP4B1 cDNAs [Gasser and Philpot, 1989; Nhamburo et al., 1989; Yokotani et al., 1990; Imaoka et al., 1995].

Isolation of the Rabbit Corneal CYP4B1 Promoter Region

A 3.41-kb DNA promoter region of the *CYP4B1* gene (GenBank accession no.: AY227450) was isolated from the rabbit corneas using the PCR-based GenomeWalker approach. Multiple 5′-RACE studies identified the start site of the rabbit corneal CYP4B1 cDNA as a guanosine residue located 33 bp upstream of the ATG start codon (Figs. 1 and 2), while the predicted transcription start site (http://www.fruitfly.org/seq_tools/promoter.html) was identified as a cytidine residue located 36bp upstream of the ATG start codon (Fig. 2). However, primer extension analysis indicated that the major transcription start site coincided with that of the guanosine residue (data not shown). A putative TATA box sequence (TATAA) was found at −30 bp relative to the beginning of the cDNA (transcription start site +1 (G)). Interestingly, the 5′-UTR of the rabbit corneal CYP4B1 mRNA is relatively short, indicating a unique feature for this gene.

The isolated 5′-flanking region of the rabbit corneal CYP4B1 was aligned to corresponding sequences in the human and mouse genome databases using DNASTAR computer software (Madison, WI). The results showed that the isolated corneal CYP4B1 promoter fragment exhibited 22% and 65% homology with the mouse and human 5′-flanking regions

Fig. 1. (*Overleaf*) Reconstructed cDNA sequence encoding the corneal CYP4B1 isoform and alignment to the known sequence of the rabbit lung CYP4B1. Lowercase text represents the nucleotide sequence of the previously defined rabbit corneal cDNA fragment [Mastyugin et al., 1999]. ATG is a start codon encoding the Methionine (M). TAG is a STOP codon. Codons *TTT* (cornea) and *TTC* (lung) encode the same amino acid phenylalanine (F). The nucleotide sequence 5′-*CCTGAGGTCTTTGACCCCCTGCGC* encodes the meander region polypeptide sequence PEVFD^{422}PLR, critical for heme binding to CYP4B1. The nucleotide sequence 5′-*TTCTCTGCCGGGCCCAGGAACTGCATCGGGCAGCAGTTC* encodes the putative heme-binding region FSAGPRNCIGQQF.

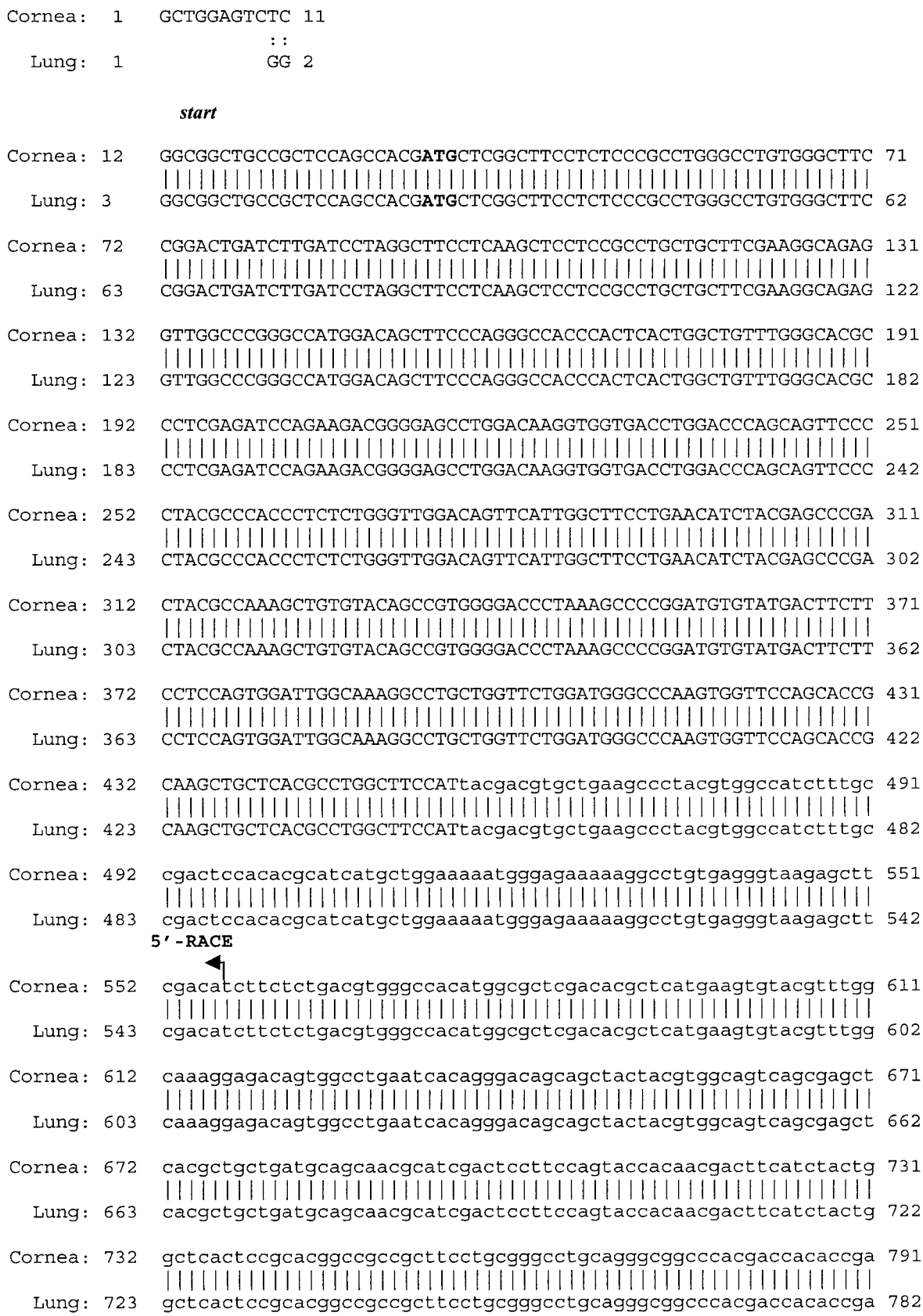
Cornea: 1 GCTGGAGTCTC 11
Lung: 1 GG 2
start
Cornea: 12 GGCGGCTGCCGCTCCAGCCACGATGCTCGGCTTCCTCTCCCGCCTGGGCCTGTGGGCTTC 71
Lung: 3 GGCGGCTGCCGCTCCAGCCACGATGCTCGGCTTCCTCTCCCGCCTGGGCCTGTGGGCTTC 62
Cornea: 72 CGGACTGATCTTGATCCTAGGCTTCCTCAAGCTCCTCCGCCTGCTGCTTCGAAGGCAGAG 131
Lung: 63 CGGACTGATCTTGATCCTAGGCTTCCTCAAGCTCCTCCGCCTGCTGCTTCGAAGGCAGAG 122
Cornea: 132 GTTGGCCCGGGCCATGGACAGCTTCCCAGGGCCACCCACTCACTGGCTGTTTGGGCACGC 191
Lung: 123 GTTGGCCCGGGCCATGGACAGCTTCCCAGGGCCACCCACTCACTGGCTGTTTGGGCACGC 182
Cornea: 192 CCTCGAGATCCAGAAGACGGGGAGCCTGGACAAGGTGGTGACCTGGACCCAGCAGTTCCC 251
Lung: 183 CCTCGAGATCCAGAAGACGGGGAGCCTGGACAAGGTGGTGACCTGGACCCAGCAGTTCCC 242
Cornea: 252 CTACGCCCACCCTCTCTGGGTTGGACAGTTCATTGGCTTCCTGAACATCTACGAGCCCGA 311
Lung: 243 CTACGCCCACCCTCTCTGGGTTGGACAGTTCATTGGCTTCCTGAACATCTACGAGCCCGA 302
Cornea: 312 CTACGCCAAAGCTGTGTACAGCCGTGGGGACCCTAAAGCCCCGGATGTGTATGACTTCTT 371
Lung: 303 CTACGCCAAAGCTGTGTACAGCCGTGGGGACCCTAAAGCCCCGGATGTGTATGACTTCTT 362
Cornea: 372 CCTCCAGTGGATTGGCAAAGGCCTGCTGGTTCTGGATGGGCCCAAGTGGTTCCAGCACCG 431
Lung: 363 CCTCCAGTGGATTGGCAAAGGCCTGCTGGTTCTGGATGGGCCCAAGTGGTTCCAGCACCG 422
Cornea: 432 CAAGCTGCTCACGCCTGGCTTCCATtacgacgtgctgaagccctacgtggccatctttgc 491
Lung: 423 CAAGCTGCTCACGCCTGGCTTCCATtacgacgtgctgaagccctacgtggccatctttgc 482
Cornea: 492 cgactccacacgcatcatgctggaaaaatgggagaaaaaggcctgtgagggtaagagctt 551
Lung: 483 cgactccacacgcatcatgctggaaaaatgggagaaaaaggcctgtgagggtaagagctt 542
5'-RACE
Cornea: 552 cgacatcttctctgacgtgggccacatggcgctcgacacgctcatgaagtgtacgtttgg 611
Lung: 543 cgacatcttctctgacgtgggccacatggcgctcgacacgctcatgaagtgtacgtttgg 602
Cornea: 612 caaaggagacagtggcctgaatcacagggacagcagctactacgtggcagtcagcgagct 671
Lung: 603 caaaggagacagtggcctgaatcacagggacagcagctactacgtggcagtcagcgagct 662
Cornea: 672 cacgctgctgatgcagcaacgcatcgactccttccagtaccacaacgacttcatctactg 731
Lung: 663 cacgctgctgatgcagcaacgcatcgactccttccagtaccacaacgacttcatctactg 722
Cornea: 732 gctcactccgcacggccgccgcttcctgcgggcctgcagggcggcccacgaccacaccga 791
Lung: 723 gctcactccgcacggccgccgcttcctgcgggcctgcagggcggcccacgaccacaccga 782

Fig. 1.

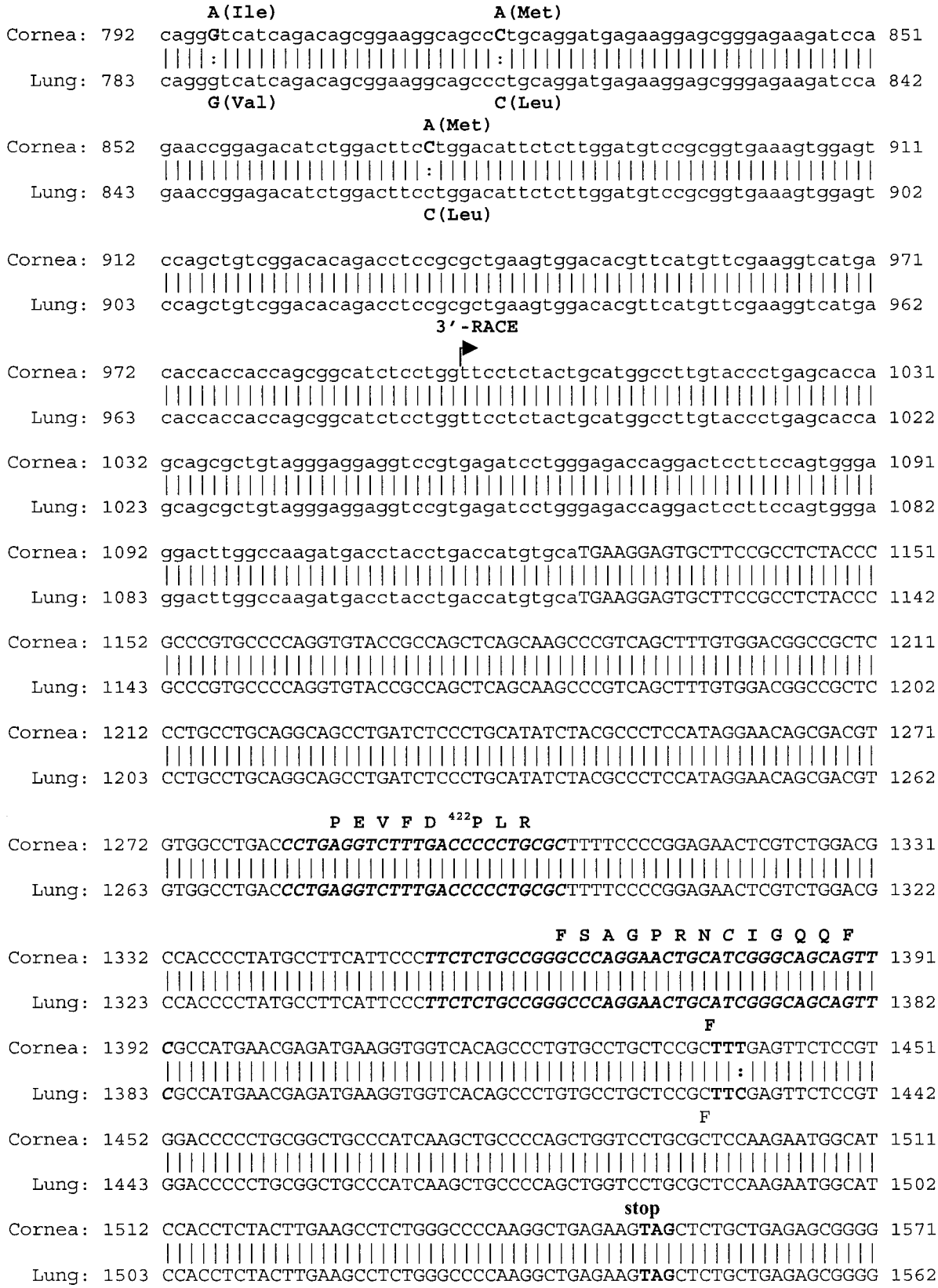

Fig. 1. (*Continued*)

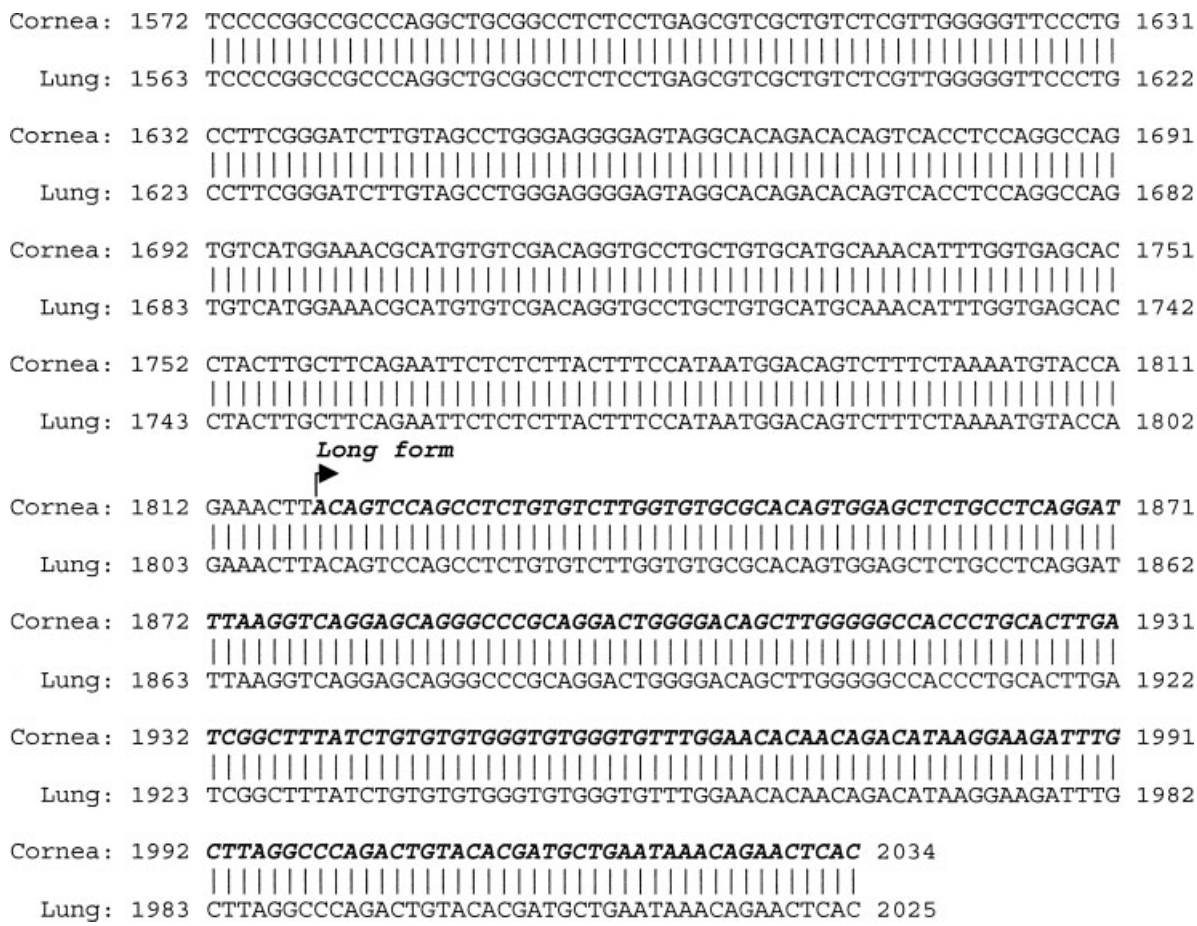

Fig. 1. (*Continued*)

(immediately upstream of the start site of the CYP4B1 cDNA), respectively.

Computer analysis of the promoter sequence revealed the presence of *cis*-acting elements including putative regulatory elements, which have been reported to be functionally related to induction of CYP proteins and to hypoxia responses. As seen in Figure 2, several DNA binding sequences were predicted for transcription factors that have been implicated in the induction of CYP4 proteins. These include preoxisomal proliferators activated receptors (PPAR/RXR heterodimer), barbiturate response factor, hepatic nuclear factor (HNF) and Ah receptor (ARNT heterodimer). With regard to hypoxia responsive elements, the CYP4B1 contains two putative HIF-1 binding sequences with 100% homology to the core consensus sequence of the HIF-1 binding site, i.e., 5′-BACGTGSB-3′ [Mazure et al., 2002]. One HIF-1 binding site is located at −865 to −858 on the sense strand and the second one is located on the antisense strand at −2195 to −2187 (Fig. 2). Another putative site with 80% of the core consensus sequence of HIF-1 binding site is located at −73 to −67, 5′-gCGTGgc-3′. Figure 2 also indicates the presence of DNA binding sites having the core consensus sequence for various transcription factors that have been implicated in the induction of numerous genes in response to hypoxia; most notably are sequences for AP-1, NFκB, Sp1, and C/EBP. The presence of these sequences could explain, at least in part, the increased mRNA levels of CYP4B1 following hypoxic injury in vitro and in vivo.

Effect of Hypoxia on CYP4B1 Promoter Activity

Five different luciferase reporter constructs containing various deletions of the isolated 3.41 kb fragment of the 5′-untranslated region of the CYP4B1 gene were made to start elucidating the molecular mechanisms underlying CYP4B1 transcriptional activation in response to injury. We used the rabbit corneal epithelial cells for transient transfection and

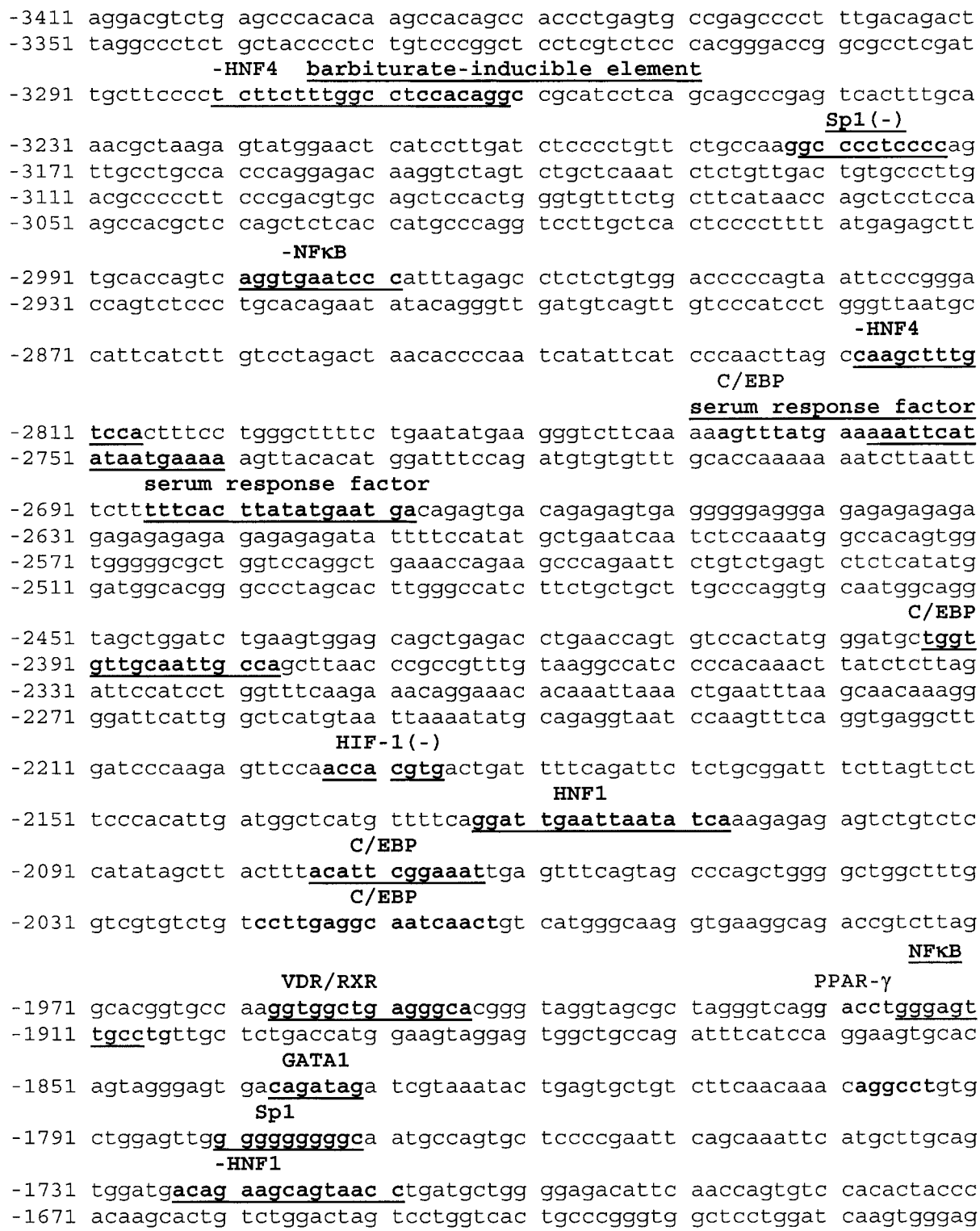

Fig. 2. Putative regulatory elements in the rabbit *CYP4B1* gene promoter. The predicted transcription start site is indicated in large font (C) and an arrow. Underlined sequences represent possible *cis*-regulatory elements: HIF-1, hypoxia-inducible factor 1; AP-1, activator protein 1; NFκB, nuclear factor p50/p65; SP1, stimulating protein 1; HNF-1, hepatic nuclear factor; PPAR, peroxisomal proliferator activated receptor; RXR, retinoic acid receptor; VDR, vitamin D receptor; C/EBP, CAAT box enhancer protein.

```
                                                                GATA-1
-1611 ctccttctgg ctctcctcca aacactccct agccaggcca gagtcaggct gataaacgaa
                                                              VDR/RXR
-1551 tcggccataa atcatgcaag tcggctgatg gcatatcgtg tttcctcatt ctccccaccct
-1491 ggggccttgc agtgaaatgg gatacccagg gtctccagcc agtgagacga ggttgaactc
-1431 cgcatttcag ggagggtgcc gagccctggg gaagacactc ctttcactgt gcttcttctt
-1371 gccgtctgcc taggggcagg cccgcatgat gtcccctcgg tggaggcagg ggcttggtct
 ELK1(CCGGAARY)    VDR/RXR          AP1(TGASTCA)
-1311 gcccggaagg ctagggaggc catgtctgtg agtcagcacc tgcagcgggg gttccaggtt
-1251 ccgctgctgc ctcccgctgg actcagcgtc tgctctttcc tcctggctgc gggcttatgc
        NFκB-like(GGGAMTTYCC)
-1191 ctgcccgggg actcaccccg gctcccatgg cagcgcgcct ttgggtacgc tgggcggatg
      NF B-like
-1131 ggagactcca gcaagagatt ggaggtggga ggggagaggg tttgggacag tttttctcta
                                                              PPAR/RXR
-1071 ctccttcgct gttctggttt aacttcacag ctgtcttccc atcgagacct cttgcccagg
-1011 ctctgggaac agcattgccg ccctattcct gcagcctagg ggtgtcgctg gggctcctgc
                                        MTF-1(-)
 -951 cgtcacaggc tctggaggct acatcatccc gtgtgcaaat ctttcactct gccatctcct
                            E-box/HIF-1(USF,ARNT homodimer)
 -891 tccaagggag cctcacgtcc aggaaacacg tggggtgaat tccatttcct gcggcgcccg
 -831 gcccgagatg gtacaggagt gggaaacagc agtctctccc tggggcatgg ggctgggcca
                              EGR-LIKE(GNTKGGGYG)
 -771 aactcgtcct tcagcagaac cctgggctgg gggcgtttga gctgccgctt ccttgctgtg
                            serum response factor
 -711 caagtgttag actcgtcccg atccctctct ggatctaagt ggccttactc acccaggagg
                      NFκB(p50)
 -651 gattggacct gcgggtctcc cctcatcacc ctaaaagtaa tgttttaatt tcctaaatgt
                              MTF-1(-)
 -591 caactaggta ctctgctttc aaggggtgca gctgggtctt tgcttaccag agatcttcct
                                        serum response factor
 -531 tccggggctt agacccacgc ctctggagat gtcccccaaa gaaggaatca gaacttcatg
                C/EBP
 -471 aggctggcat ggggcaagcc ctcctgaag gccacatgga aggggacagt gggaactttc
        GATA-1
 -411 ttgtgataaa gcatgggcaa gttgcacctc cattttatta tccgagaaat gggtattcag
                                                      HNF1-like
 -351 aatgagtacc tatgatctcc tgttgtcccg gttaaatggg ttaatgtgta aaaaatgcct
   barbiturate-inducible element
 -291 gtagggaaag gcagcggcta tcatgctgaa aattacacca agagctgccc cctacgggct
                EGR-LIKE(GNTKGGGYG)
 -231 cccccaagga atcaaggtgg ggtgcccacg cctagcatgc ttttaactga gttttgggaa
 -171 aagtcagcca agttctcacc tctgttgccg gtgatttttg gggttgctgt ctcctccctg


                                                  HIF-1-like(XRE)
-111 tggcactcag cccgggctgg gctgctgctg gctgcagggc gtggcgaggg gtgggagctg
                                                                CYP4B1 cDNA
                                    TATA box                        ▶
 -51 gcggggcgcc tgggttcaga gtataagaga agccagggac agcgggagaC aaGCTGGAGT
   9 CTCGGCGGCT GCCGCTCCAG CCACGATGCT CGGCTTCCTC TCCCGCCTGG GCCTGTGGGC
  69 TTCCGG
```

Fig. 2. (*Continued*)

promoter activity analysis. Transfection with the −640/+22, −955/+22, −1787/+22, and −3435/+22 constructs resulted in a significant induction of CYP4B1 transcriptional activity in response to hypoxia (Fig. 3). The highest increase (2-fold) in transcriptional activity was detected with the −640/+22 construct and may reflect the presence of an NFκB binding site that is not present in the −194/+22 construct. The −194/+22 luciferase construct produced high levels of transcriptional activity in RCE cells under hypoxic conditions, but was not significantly different compared to normoxic conditions (Fig. 3). The −194/+22 construct contains an HIF-1-like (XRE) binding site located close to the putative TATA-box element. It may not be sufficient for a significant increase in induction of the *CYP4B1* gene in response to hypoxia.

The xenobiotic compound 3-MC activates the transcription of certain P-450 genes via the transcription factor aryl hydrocarbon receptor (AhR). Upon activation, AhR forms a heterodimer with another transcription factor ARNT [Pollenz et al., 1999]. The activation of AhR-ARNT may constitute a mechanism for the induction of CYP4B1 since 3-MC also stimulates the formation of 12(*R*)-HETE and 12(*R*)-HETrE in the corneal epithelium [Mastyugin et al., 1999]. CYP4B1 promoter activity in RCE cells transfected with the luciferase constructs −194/+22, −955/+22, and −3435/+22 increased by 2–3-fold following exposure to 3-MC. The activity of these constructs to both, hypoxia and 3-MC, was not different from the response to 3-MC alone. Conversely, promoter activity of the −1787/+22 construct decreased in response to 3-MC but exposure to hypoxia reversed the 3-MC effect on the −1787/+22 construct-derived activity (Fig. 4). The presence of a certain combination of *cis*-elements in −1787/+22 construct and absence of such a set in the −955/+22 construct might produce transcriptional inhibitory complex, while exposure to hypoxia might produce rearrangement of transcriptional complex due to activation of two NFκB-like sites and AP-1 site in the −1787/+22 construct. On the other hand, the −194/+22 construct, which did not respond to hypoxia (Fig. 3), showed a twofold increase in transcriptional activity in respond to 3-MC (Fig. 4), suggesting that this HIF-1-like (XRE) binding site exhibits higher affinity to xenobiotics, AhR ligands.

Involvement of HIF-1, AP-1, and NFκB in the Hypoxia-Induced Transcription of CYP4B1

As indicated above, the isolated CYP4B1 promoter fragment contains three putative binding sites for the HIF-1 transcription factor. We performed EMSA on nuclear extracts from RCE cells exposed to hypoxia using the HIF-1 putative DNA binding sequences of the CYP4B1 to further evaluate the contribution of HIF-1 to hypoxia-induced CYP4B1 expression. As seen in Figure 5, nuclear binding activity for the ^{32}P-labeled HIF-1 probe from the CYP4B1 promoter (−871 to −852) showed a strong 5- and 6-fold increase in cells exposed to 1 and 4 h of hypoxia, respectively. This binding activity was due to sequence-specific binding to the HIF-1 oligonucleotide probe as shown by competition with excess unlabeled probe for the HIF-1 (Fig. 6). Nuclear binding activity was also detected using a ^{32}P-labeled oligonucleotide that codes for the putative site having 80% of the core consensus sequence of HIF-1 binding site at −73 to −67. Binding activity to this site was evident albeit much weaker. Supershift assay using antibodies against HIF-1α clearly indicated that the binding activity detected with both probes consisted of HIF-1α (Fig. 5).

We also examined the possible involvement of AP-1 and NFκB binding sites in the hypoxia induction of CYP4B1 expression. Nuclear binding activity for the ^{32}P-labeled AP-1 probe from the CYP4B1 promoter (−1290 to −1272) was present in RCE cells under normoxia and was significantly increased following 4 h exposure to hypoxia (Fig. 6). This binding activity was due to sequence-specific binding to the AP-1 oligonucleotide probe as shown by competition with a 100 molar excess unlabeled AP-1 probe but not with an excess of unlabeled NFκB probe. Supershift assay indicated that the binding activity was composed of c-fos protein (Fig. 6).

EMSA of RCE nuclear extracts using the ^{32}P-labeled NFκB probe from the CYP4B1 promoter (−1136 to −1112) showed a marked increase in binding activity following exposure to hypoxia for 1 and 4 h of about fourfold over the control normoxic condition (Fig. 7). This binding activity was due to sequence-specific binding to the NFκB oligonucleotide probe as evidenced by competition with excess unlabeled probe for the NFκB but not with unlabeled probe for AP-1. Supershift assay using antibodies against p50

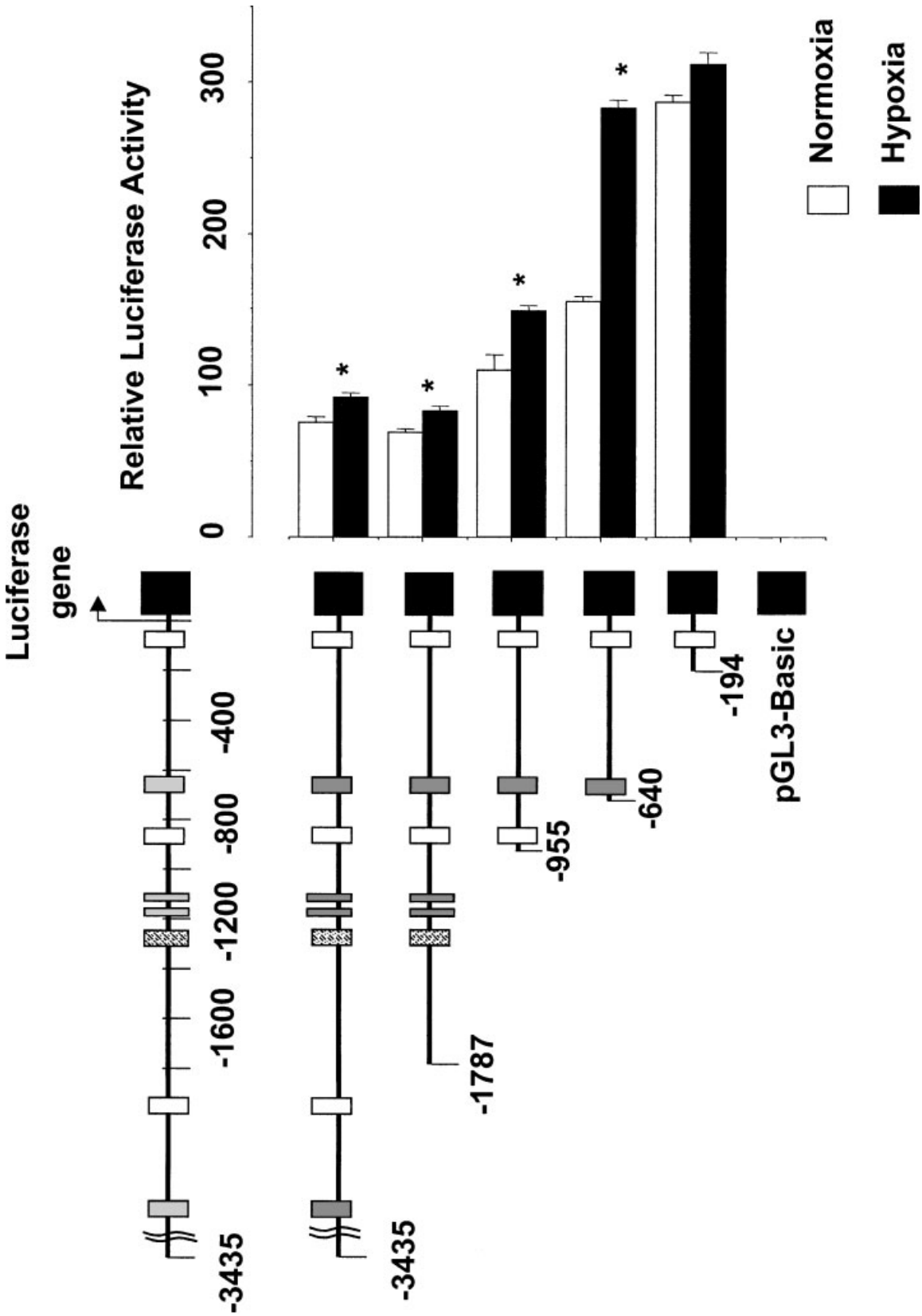

Fig. 3. Effect of hypoxia on CYP4B1 promoter activity in RCE cells. Transfected cells were cultured in normoxia or hypoxia for 24 h. Firefly luciferase activity is expressed relative to the Renilla luciferase activity. The results are the mean ± SE; n = 5; $*P < 0.05$ from corresponding normoxia. The putative binding sites for HIF-1, NFκB, and AP-1 are represented by open, gray, and hatched bars, respectively.

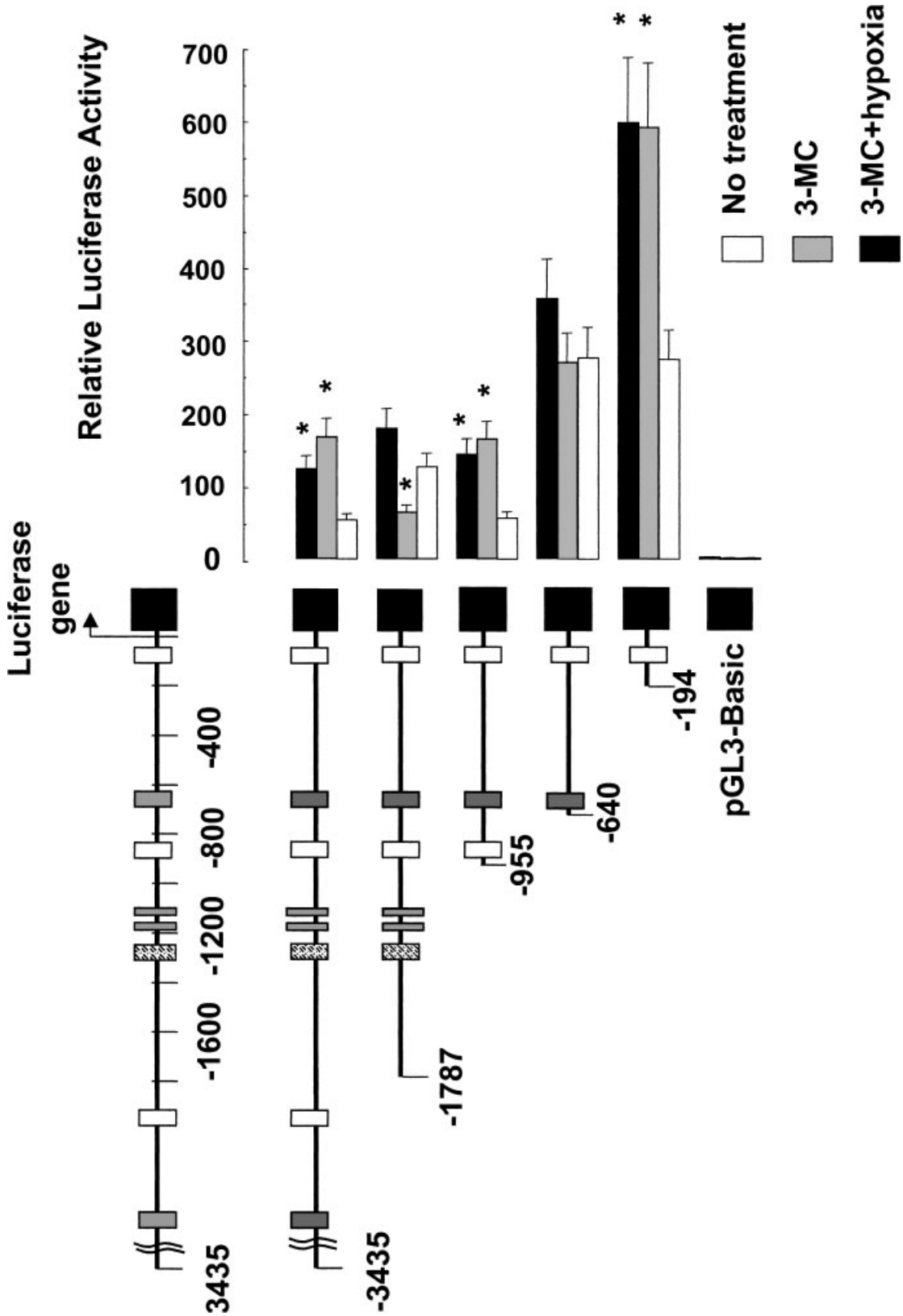

Fig. 4. Effect of 3-MC and hypoxia on CYP4B1 promoter activity in RCE cells. Transfected cells were cultured in normoxia or hypoxia in the presence and absence of 3-MC (2 μM) for 24 h. Firefly luciferase activity is expressed relative to the Renilla luciferase activity. The results are the mean ± SE; n = 4; $^*P < 0.05$ from corresponding control. The putative binding sites for HIF-1, NFκB, and AP-1 are represented by open, gray, and hatched bars, respectively.

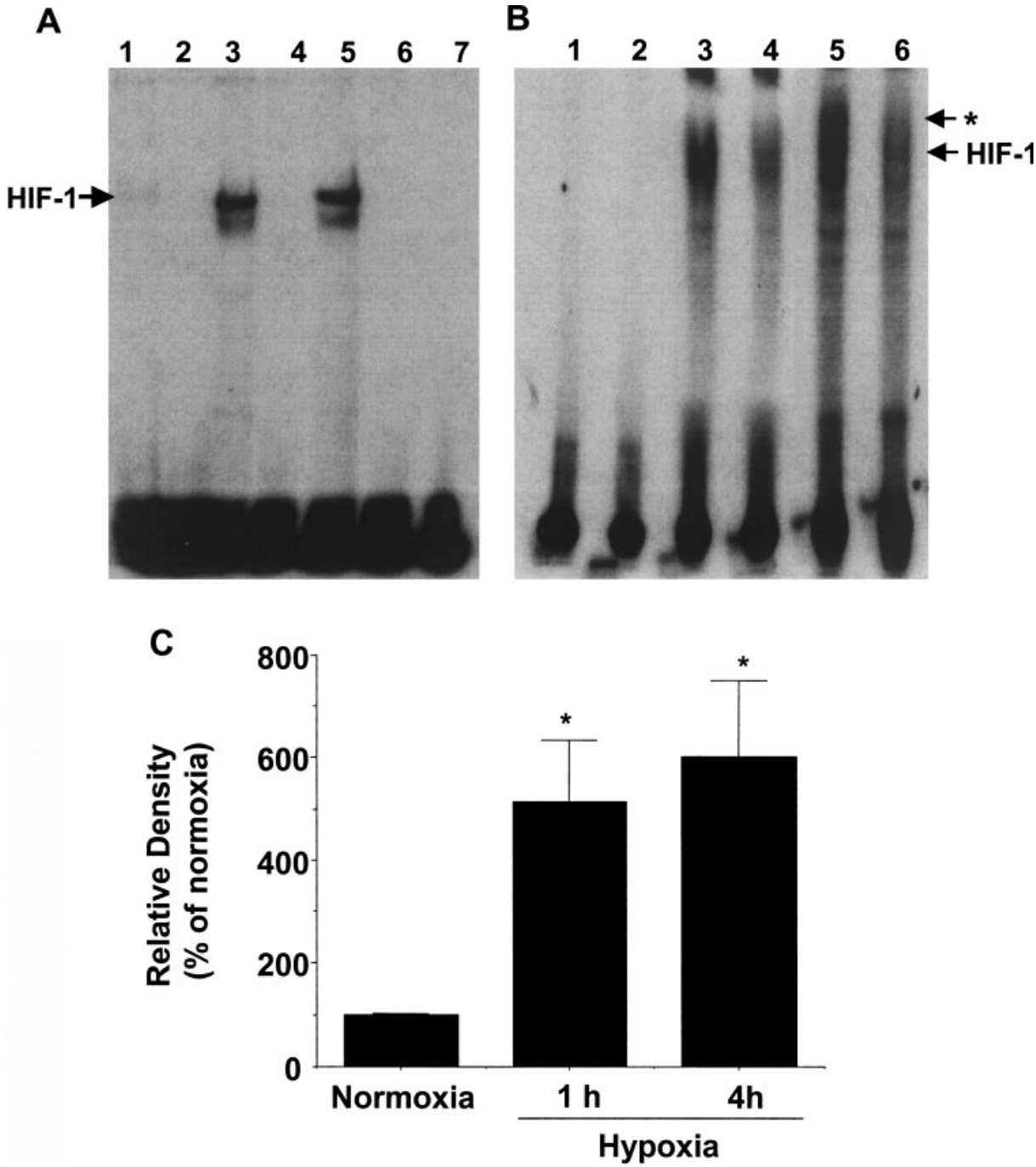

Fig. 5. Hypoxia-mediated increase of nuclear binding activity for HIF-1 in RCE cells. **A**: EMSA with CYP4B1-HIF-1 binding sequence (−871 to −852; 5′-aggaaaCACGTGGGgtgaat-3′) and nuclear extracts from cells incubated under normoxia (**lanes 1** and **2**) or hypoxic conditions for 1 h (**lanes 3** and **4**) and 4 h (**lanes 5** and **6**) in the absence (lanes 1, 3, and 5) and presence (lanes 2, 4 and 6) of an excess of unlabeled HIF-1 probe; **lane 7**, free probe, no nuclear extract. **B**: Supershift assay. EMSA was performed using nuclear extracts from cells incubated under hypoxic (**lanes 3–6**) conditions and ^{32}P-labeled double stranded oligonucleotides for the binding sites of HIF-1 at −871 to −851 (lanes 3 and 5) and at −73 to −69 (lanes 4 and 6) in the absence (lanes 3 and 4) and presence (lanes 5 and 6) of antibody against HIF-1α. *supershift; lanes 1 and 2, free probe. **C**: Densitometry analysis (mean ± SE, n = 4, $^*P < 0.05$).

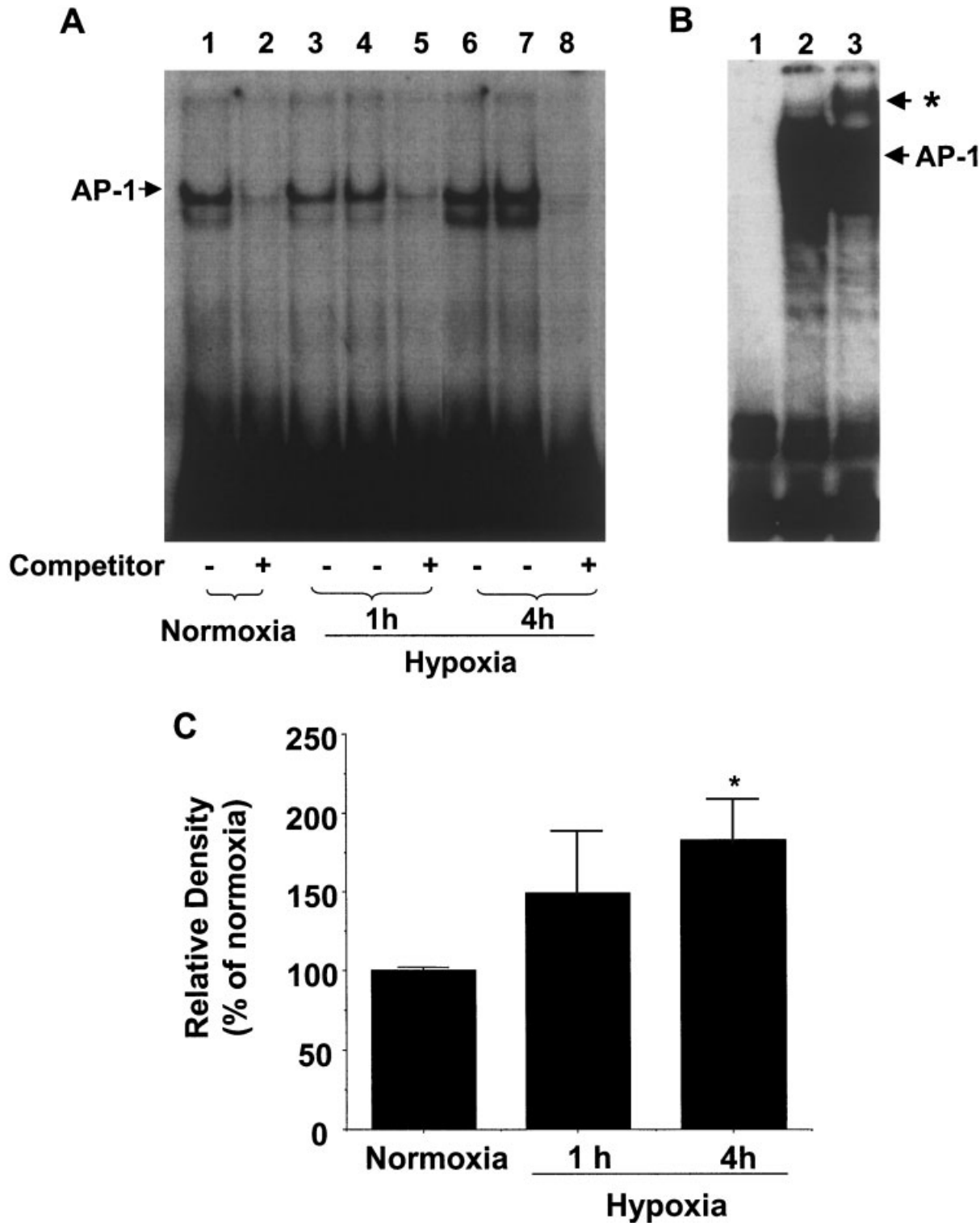

Fig. 6. Hypoxia-mediated enhancement of nuclear binding activity of AP-1 in RCE cells. **A**: EMSA with a ^{32}P-labeled double stranded oligonucleotide containing the consensus DNA binding sequence within the CYP4B1 promoter for AP-1 (−1290 to −1272; 5′-atgtctgTGAGTCAgcacc-3′), and nuclear extracts from cells incubated under normoxic and hypoxic conditions for 1 and 4 h. S, specific competitor-unlabeled AP-1 probe; NS, non-specific competitor-unlabeled NFκB probe. **B**: Supershift assay. EMSA was performed with nuclear extracts from cells incubated under hypoxic conditions and in the absence (**lane 2**) and presence (**lane 3**) of antibody against c-fos. **Lane 1**, free probe; *supershift. **C**: Densitometry analysis (mean ± SE, n = 5, $^*P < 0.05$).

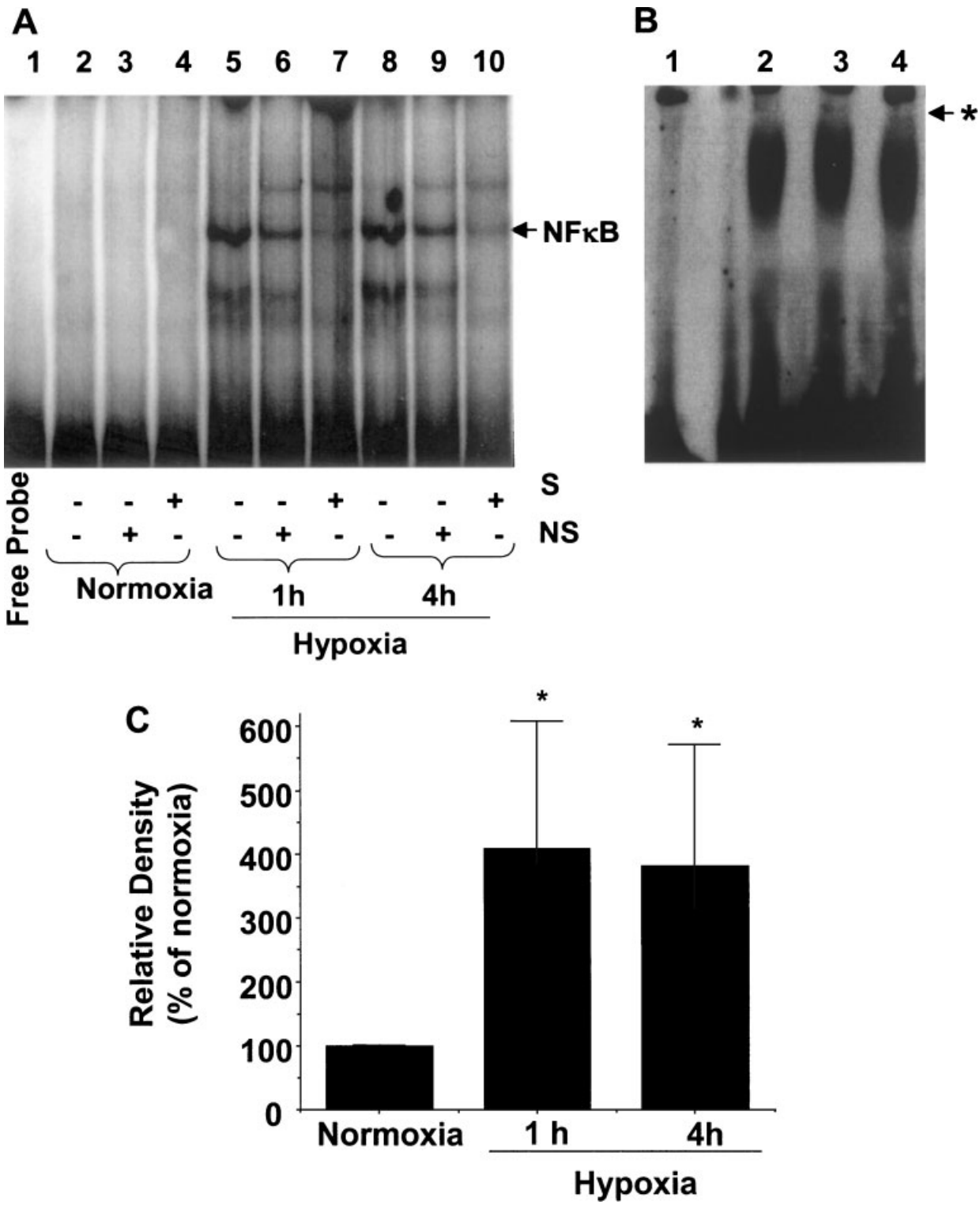

Fig. 7. Hypoxia-mediated enhancement of nuclear binding activity of NFκB in RCE cells. **A**: EMSA was performed with ^{32}P-labeled double-stranded oligonucleotides containing consensus DNA binding sequences within the CYP4B1 promoter for NFκB (−1136 to −1112; 5′-ggaTGGGAGACTCCagcaagagatt-3′) and nuclear extracts from the cells incubated under normoxic and hypoxic conditions for 1 and 4 h. Free probe, no nuclear extracts; S, specific competitor-unlabeled NFκB probe; NS, non-specific competitor-unlabeled AP-1 probe. **B**: Supershift assay. EMSA of nuclear extracts from hypoxia-treated cells in the absence (**lane 4**) and presence of antibodies against p65 (**lane 2**) or p50 (**lane 3**). **Lane 1**, free probe; *supershift. **C**: Densitometry analysis (mean ± SE, n = 3, $^*P < 0.05$).

and p65 indicated that the binding activity was composed of these proteins (Fig. 7).

DISCUSSION

The present study describes the isolation and initial analysis of the 5′-untranslated region of the corneal epithelial *CYP4B1* gene; mRNA expression of this gene is induced following hypoxic injury and the activity of its protein product is involved in the production of potent inflammatory eicosanoids. The initial analysis of the isolated 3.4 kb fragment of the CYP4B1 promoter indicated the presence of binding sequences for hypoxia-sensitive transcription factors including HIF-1, AP-1, and NFκB suggesting that binding of these factors to the CYP4B1 promoter sequences involves, at least in part, the mechanism by which hypoxia increased CYP4B1 mRNA in the corneal epithelium. Promoter activity of luciferase reporter constructs as well as EMSA with the CYP4B1 binding sequences of these factors in RCE cells subjected to hypoxia further supports this notion.

Increased transcription of various genes by hypoxia is primarily attributed to activation of the hypoxia-inducible transcription factor HIF and its binding to corresponding *cis*-elements (HREs) on the promoter region. HIF-1 was the first hypoxia-inducible transcription factor to be identified [Semenza et al., 1997]. Its activation leads in most chronic responses to hypoxic conditions to increased transcription of genes encoding erythropoietin, glucose transporters, glycolytic enzymes, vascular endothelial growth factor (VEGF), VEGF receptors, and other genes whose expression facilitate delivery of oxygen and/or produce metabolic adaptation to hypoxia [Semenza, 2000]. HIF-1 is a heterodimer composed of hypoxia-inducible HIF-1α and the constitutively expressed HIF-1β, which is also known as aryl hydrocarbon nuclear translocator (ARNT). Computer analysis of the CYP4B1 promoter predicted two putative DNA binding sites for HIF-1 having the consensus sequence 5′-B<u>ACGTG</u>SB-3′ [Semenza et al., 1997] and one upstream close to the TATA box that display 80% sequence similarity. These HIF binding sites may confer, at least in part, the molecular mechanisms by which CYP4B1 expression is increased following hypoxic injury in vitro and in vivo. Our results with the luciferase reporter genes suggested the involvement of these sites. That HIF-1 may constitute a mechanism for hypoxia induction of CYP4B1 expression is further suggested from the demonstration of a strong nuclear binding activity with the ^{32}P-labeled HIF-1 probes from the CYP4B1 promoter in response to hypoxia that was composed of HIF-1α as demonstrated by supershift assays. To our knowledge, this is the first demonstration of functional HIF-1 binding sites on a CYP gene. The effect of hypoxia on CYP expression and activity was primarily studied with hepatic CYP proteins. Hypoxia has been shown to downregulate hepatic CYP proteins by mechanisms that are thought to be mediated through increased cytokine levels [Morgan, 1993] and to an activated HIF-1 (HIF-1α/ARNT) leading to a decrease in the AhR/ARNT heterodimer for the expression of some CYP proteins [Park, 1999]. A study by Fradette et al. [2002] demonstrated increased expression of CYP3A6 in response to hypoxia in vivo in rabbit hepatocytes and suggested that hypoxia facilitates HIF-1 cooperation with nuclear factors such as GR, HNF-4, and RXR [Bunn et al., 1998; Kambe et al., 2000], which then contribute to transcriptional activation of the CYP3A6. This scenario may be operational in the case of the corneal CYP4B1 induction following hypoxic injury. However, the demonstration of a functional HIF-1 binding site provides an additional mechanistic explanation for hypoxia-induced expression of CYP4B1. The corneal *CYP4B1* gene may be under distinct molecular control that is tissue-specific and is driven by unique molecular mechanisms that include HIF-1 that is readily activated by hypoxic injury. However, additional experiments are needed to substantiate the role of HIF-1 in the hypoxia-induced expression of CYP4B1.

It is interesting to note that ARNT (HIF-1β) forms a heterodimer with the AhR transcription factor that is readily induced by aryl hydrocarbon compounds; this heterodimer activates transcription of numerous CYP genes. Thus, the mechanisms underlining the induction of CYP isoforms by xenobiotics and hypoxia may be linked via ARNT (HIF-1β). We and others have previously showed that 3-MC and β-NF, exogenous ligands of AhR, stimulates the formation of 12(*R*)-HETE and 12(*R*)-HETrE [Asakura and Shichi, 1992; Asakura et al., 1994; Mastyugin et al., 1999]. In this study, we further demonstrated that 3-MC caused activation of *CYP4B1* gene transcription. However,

exposure of 3-MC-treated cells to hypoxia did not yield a further increase in CYP4B1 promoter activity. This suggests that hypoxia and AhR ligands share a common mechanism for induction of corneal CYP4B1 expression. It also further corroborates our previous data that the enzymatic activity ascribed to CYP4B1 is not increased when hypoxia-treated corneas are exposed to the AhR ligands, 3-MC and β-NF [Mastyugin et al., 1999]. Numerous studies have demonstrated that hypoxia and the AhR ligand compete for the recruitment of the ARNT transcription factor [Gradin et al., 1996; Kim and Sheen, 2000]. Moreover, AhR ligands have been shown to suppress AP-1 and NFκB activation [Tian et al., 1999; Suh et al., 2002]. In as much as activation of NFκB and AP-1 may contribute to hypoxia induction of CYP4B1 expression, addition of AhR ligands may diminish the response to hypoxia.

The induction of CYP4B1 by hypoxia may involve other oxygen-sensitive transcription factors either directly by facilitating/augmenting HIF-1-activated transcription. Factors such as NFκB, AP-1 [Koong et al., 1994; Mukhopadhyay et al., 1995], and NF-IL-6 [Yan et al., 1997] have been implicated in the hypoxia-induced expression of various genes. A recent study by Teng et al. [2002] demonstrated that the transcription factor C/EBP-β mediates induction of the inducible nitric oxide synthase (iNOS) by hypoxia in pulmonary microvascular smooth muscle cells. Green et al. [2001] showed a central role for the metal transcription factor-1 (MRF-1) in the hypoxia induction of placenta growth factor in fibroblasts. Xu et al. [2000] described how Sp1 synergistically enhanced cyclooxygenase-2 (COX-2) promoter activity with hypoxia in the vascular endothelium. The transcription factor Egr-1 has been shown to mediate hypoxia-induced transcription of IGF-II [Bae et al., 1999]. As indicated in Figure 4, the computer analysis of the CYP4B1 promoter contains consensus sequences for some of these factors. Their contribution to *CYP4B1* gene induction needs to be explored. Our studies using nuclear extracts isolated from RCE cells and labeled probes containing the putative CYP4B1 binding sequences for AP-1 and NFκB demonstrated a marked increase in binding activity of these probes to nuclear extracts from RCE cells exposed to hypoxia. These results support a role for these transcription factors in the hypoxia induction of CYP4B1 expression. Interestingly, a recent study indicated the presence of AP-1 and Sp1 binding sites on the mouse CYP4B1 promoter [Isern and Meseguer, 2003]. However, it is unknown if the mouse CYP4B1 is regulated by hypoxia. To this end, computer analysis showed little homology (22%) between the mouse promoter fragment and that of the rabbit cornea described here.

Another possible mechanism that may account for induction or amplification of CYP4B1 expression in the corneal epithelium following injury may include the involvement of peroxisomal proliferator-activated receptors (PPARs). The transcription of many of the CYP4 genes is activated by PPARs. These endogenous nuclear receptors are activated upon bindings of exogenous ligands such as clofibrate or endogenous ligands including eicosanoids such as prostaglandins, HETEs and ω-alcohol EETs [Kliewer et al., 1997]. Yu et al. [1995] showed that cyclooxygenase-derived prostaglandins including PGD_2, PGA_2, and PGJ_2, bind to PPAR subtypes (α, δ, γ) with different specificities. On the other hand, lipoxygenase-derived hydroxy acids including 8(*S*)-HETE and leukotriene B_4 (LTB4) have been shown to be potent ligands for PPARα [Devchand et al., 1996]. Cowart et al. [2002] demonstrated that the ω-alcohol of EETs activated human and mouse PPARα in transient transfection assays suggesting these metabolites as endogenous ligands of this nuclear receptor. Hypoxia as well as inflammatory conditions may rapidly induce enzymes involved in the synthesis of these eicosanoids which in turn initiates a cascade of cellular processes leading to induction of CYP4B1 via activation of PPARs. The activation of PPARs may contribute to the expression of CYP4B1 since the exogenous ligands for this nuclear receptor, for example, clofibrate, also stimulates the formation of 12(*R*)-HETE and 12(*R*)-HETrE in the corneal epithelium and increases the levels of CYP4B1 in RCE cells [Mastyugin et al., 1999]. We have demonstrated that RCE cells do express transcripts for PPARα and PPARβ but not for PPARγ [Bonazzi et al., 2000]. Computer analysis of the CYP4B1 promoter suggested the presence of a PPAR/RXR heterodimer binding site located at −1027 to −1007 as well as a PPARγ binding site at −1922 to −1906. Preliminary data indicate that clofibrate also increases CYPP4B1 promoter activity in transient transfection experiments, further suggesting the contribution of

PPAR ligands to the transcriptional activation of CYP4B1.

In summary, the present study reports the isolation, characterization, and initial analysis of the corneal CYP4B1 full-length cDNA and 3.4 kb of the promoter region. The results substantiate previous data that the corneal *CYP4B1* is a hypoxia-inducible gene whose expression is rapidly increased following hypoxic injury in vitro and in vivo. This hypoxia inducibility may be a distinctive feature of the corneal CYP4B1. The corneal epithelium is routinely challenged by prolonged period of hypoxia during eyelid closure while asleep, something that the lung never experiences. Hypoxia caused by eye closure creates an inflammatory response as well [Sack et al., 1992]; it is also a condition where the levels of CYP-derived eicosanoids are significantly elevated [Conners et al., 1995b; Vafeas et al., 1998]. The unique sequences on the promoter of the CYP4B1 allow rapid response to changes in oxygen tension.

REFERENCES

Araki K, Ohashi Y, Kinoshita S, Hayashi K, Yang XZ, Hosaka Y, Aizawa S, Handa H. 1993. Immortalization of rabbit corneal epithelial cells by a recombinant SV40-adenovirus vector. Invest Ophthalmol Vis Sci 34:2665–2671.

Asakura T, Shichi H. 1992. 12(*R*)-hydroxyeicosatetraenoic acid synthesis by 3-methylcholanthrene- and clofibrate-inducible cytochoem P450 in porcine ciliary epithelium. Biochem Biophys Res Commun 187:455–459.

Asakura T, Matsuda M, Matsuda S, Shichi H. 1994. Synthesis of 12(*R*) and 12(*S*)-hydroxyeicosatetraenoic acid by porcine ocular tisssue. J Ocul Pharm 10:525–536.

Bae SK, Bae MH, Ahn MY, Son MJ, Lee YM, Bae MK, Lee OH, Park BC, Kim KW. 1999. Egr-1 mediates transcriptional activation of IGF-II gene in response to hypoxia. Cancer Res 59:5989–5994.

Bonazzi A, Mastyugin V, Mieyal PA, Dunn MW, Laniado Schwartzman M. 2000. Regulation of cyclooxygenase-2 by hypoxia and PPAR ligands in the rabbit corneal epithelium. J Biol Chem 275:2837–2844.

Bunn HF, Gu J, Huang LE, Park JW, Zhu H. 1998. Erythropoietin: A model system for studying oxygen-dependent gene regulation. J Exp Biol 201:1197–1201.

Conners MS, Stoltz RA, Dunn MW, Levere RD, Abraham NG, Schwartzman ML. 1995a. A closed eye-contact lens model of corneal inflammation. II. Inhibition of cytochrome P450 arachidonic acid metabolism alleviates inflammatory sequelae. Invest Ophthalmol Vis Sci 36: 841–850.

Conners MS, Stoltz RA, Webb SC, Rosenberg J, Dunn MW, Abraham NG, Schwartzman ML. 1995b. A closed eye-contact lens model of corneal inflammation. I. Induction of cytochrome P450 arachidonic acid metabolism. Invest Ophthalmol Vis Sci 36:828–840.

Conners MS, Urbano F, Vafeas C, Stoltz RA, Dunn MW, Laniado Schwartzman M. 1997. Alkali burn-induced synthesis of inflammatory eicosanoids in rabbit corneal epithelium. Invest Ophthalmol Vis Sci 38:1963–1971.

Cowart LA, Wei S, Hsu MH, Johnson EF, Krishna MU, Falck JR, Capdevila JH. 2002. The CYP4A isoforms hydroxylate epoxyeicosatrienoic acids to form high affinity peroxisome proliferator-activated receptor ligands. J Biol Chem 277:35105–35112.

Devchand PR, Keller H, Peters JM, Vazquez M, Gonzalez FJ, Wahli W. 1996. The PPARa-leukotriene B_4 pathway to inflammation control. Nature 384:39–43.

Fradette C, Bleau AM, Pichette V, Chauret N, Du Souich P. 2002. Hypoxia-induced down-regulation of CYP1A1/1A2 and up-regulation of CYP3A6 involves serum mediators. Br J Pharmacol 137:881–891.

Gasser R, Philpot RM. 1989. Primary structures of cytochrome P-450 isozyme 5 from rabbit and rat and regulation of species-dependent expression and induction in lung and liver: Identification of cytochrome P-450 gene subfamily IVB. Mol Pharmacol 35:617–625.

Gradin K, McGuire J, Wenger RH, Kvietikova I, Whitelaw ML, Toftgard R, Tora L, Gassmann M, Poellinger L. 1996. Functional interference between hypoxia and dioxin signal transduction pathways: Competition for recruitment of the Arnt transcription factor. Mol Cell Biol 16:5221–5231.

Green CJ, Lichtlen P, Huynh NT, Yanovsky M, Laderoute KR, Schaffner W, Murphy BJ. 2001. Placenta growth factor gene expression is induced by hypoxia in fibroblasts: A central role for metal transcription factor-1. Cancer Res 61:2696–2703.

Imaoka S, Hiroi T, Tamura Y, Yamazaki H, Shimada T, Komori M, Degawa M, Funae Y. 1995. Mutagenic activation of 3-methoxy-4-aminoazobenzene by mouse renal cytochrome P450 CYP4B1: Cloning and characterization of mouse CYP4B1. Arch Biochem Biophys 321: 255–262.

Isern J, Meseguer A. 2003. Hormonal regulation and characterisation of the mouse *Cyp4b1* gene 5′-flanking region. Biochem Biophys Res Commun 307:139–147.

Kambe T, Tada-Kambe J, Kuge Y, Yamaguchi-Iwai Y, Nagao M, Sasaki R. 2000. Retinoic acid stimulates erythropoietin gene transcription in embryonal carcinoma cells through the direct repeat of a steroid/thyroid hormone receptor response element half-site in the hypoxia-response enhancer. Blood 96:3265–3271.

Kim JE, Sheen YY. 2000. Inhibition of 2,3,7,8-tetrachlorodibenzo-*p*-dioxin (TCDD)-stimulated Cyp1a1 promoter activity by hypoxic agents. Biochem Pharmacol 59:1549–1556.

Kliewer SA, Sundseth SS, Jones SA, Brown PJ, Wisely GB, Koble CS, Devchand P, Wahli W, Willson TM, Lenhard JM, Lehmann JM. 1997. Fatty acids and eicosanoids regulate gene expression through direct interactions with peroxisome proliferator-activated receptors alpha and gamma. Proc Natl Acad Sci USA 94:4318–4323.

Koong AC, Chen EY, Giaccia AJ. 1994. Hypoxia causes the activation of nuclear factor κB through the phosphorylation of IkB on tyrosine residues. Can Res 54:1425–1430.

Laniado Schwartzman M. 1997. Cytochrome P450 and arachidonic acid metabolism in the corneal epithelium: Role in inflammation. In: Green K, Edelhauser HF,

Hackett RB, Hull DS, Potter DE, Tripathi RC, editors. Advances in ocular toxicology. New York, NY: Plenum Press, pp 3–20.

Laniado-Schwartzman M, Lavrovsky Y, Stoltz RA, Conners MS, Falck JR, Chauhan K, Abraham NG. 1994. Activation of nuclear factor κB and oncogene exoression by 12(*R*)-hydroxyeicosatrienoic acid, an angiogenic factor in microvessel endothelial cells. J Biol Chem 269:24321–24327.

Mastyugin V, Aversa E, Vafeas C, Mieyal P, Laniado Schwartzman M. 1999. Hypoxia-induced production of 12-hydroxyeicosanoids in the corneal epithelium: Involvement of a CYP4B1 isoform. J Pharmacol Exp Ther 289:1611–1619.

Mastyugin V, Mosaed S, Bonazzi A, Dunn MW, Laniado-Schwartzman M. 2001. Corneal epithelial VEGf and cytochrome P450 4B1 expression in a rabbit model of closed eye contact lens wear. Curr Eye Res 23:1–10.

Mazure NM, Chauvet C, Bois-Joyeux B, Bernard MA, Nacer-Cherif H, Danan JL. 2002. Repression of alpha-fetoprotein gene expression under hypoxic conditions in human hepatoma cells: Characterization of a negative hypoxia response element that mediates opposite effects of hypoxia inducible factor-1 and c-Myc. Cancer Res 62: 1158–1165.

Mieyal PA, Dunn MW, Schwartzman ML. 2001. Detection of endogenous 12-hydroxyeicosatrienoic acid in human tear film. Invest Ophthalmol 42:328–332.

Morgan ET. 1993. Down-regulation of multiple cytochrome P450 gene products by inflammatory mediators in vivo. Biochem Pharmacol 45:415–419.

Mukhopadhyay D, Tsiokas L, Zhou XM, Foster D, Brugge JS, Sukhatme VP. 1995. Hypoxic induction of human vascular endothelial growth factor expression through c-Src activation. Nature 375:577–581.

Nhamburo PT, Gonzalez FJ, McBride OW, Gelboin HV, Kimura S. 1989. Identification of a new P450 expressed in human lung: Complete cDNA sequence, cDNA-directed expression and chromosome mapping. Biochem 28:8060–8066.

Park H. 1999. Aromatic hydrocarbon nuclear translocator as a common component for the hypoxia- and dioxin-induced gene expression. Mol Cells 9:172–178.

Pollenz RS, Davarinos NA, Shearer TP. 1999. Analysis of aryl hydrocarbon receptor-mediated signaling during physiological hypoxia reveals lack of competition for the aryl hydrocarbon nuclear translocator transcription factor. Mol Pharmacol 56:1127–1137.

Sack RA, Tan KO, Tan A. 1992. Diurnal tear cycle: Evidence of a nocturnal inflammatory constitutive tear fluid. Invest Ophthalmol Vis Sci 33:626–640.

Semenza GL. 2000. HIF-1: Mediator of physiological and pathophysiological responses to hypoxia. J Appl Physiol 88:1474–1480.

Semenza GL, Agani F, Booth G, Forsythe J, Iyer N, Jiang BH, Leung S, Roe R, Wiener C, Yu A. 1997. Structural and functional analysis of hypoxia-inducible factor 1. Kidney Int 51:553–555.

Suh J, Jeon YJ, Kim HM, Kang JS, Kaminski NE, Yang KH. 2002. Aryl hydrocarbon receptor-dependent inhibition of AP-1 activity by 2,3,7,8-tetrachlorodibenzo-*p*-dioxin in activated B cells. Toxicol Appl Pharmacol 181:116–123.

Teng X, Li D, Catravas JD, Johns RA. 2002. C/EBP-beta mediates iNOS induction by hypoxia in rat pulmonary microvascular smooth muscle cells. Circ Res 90:125–127.

Tian Y, Ke S, Denison MS, Rabson AB, Gallo MA. 1999. Ah receptor and NF-kappaB interactions, a potential mechanism for dioxin toxicity. J Biol Chem 274:510–515.

Vafeas C, Mieyal PA, Urbano F, Falck JR, Chauhan K, Berman M, Laniado Schwartzman M. 1998. Hypoxia stimulates the synthesis of cytochrome P450-derived inflammatory eicosanoids in rabbit corneal epithelium. J Pharmacol Exp Ther 287:903–910.

Xu Q, Ji YS, Schmedtje JF, Jr. 2000. Sp1 increases expression of cyclooxygenase-2 in hypoxic vascular endothelium. Implications for the mechanisms of aortic aneurysm and heart failure. J Biol Chem 275:24583–24589.

Yan SF, Zou YS, Mendelsohn M, Gao Y, Naka Y, Du Yan S, Pinsky D, Stern D. 1997. Nuclear factor interleukin 6 motifs mediate tissue-specific gene transcription in hypoxia. J Biol Chem 272:4287–4294.

Yokotani N, Sogawa K, Matsubara S, Gotoh O, Kusunose E, Kusunose M, Fujii-Kuriyama Y. 1990. cDNA cloning of cytochrome P-450 related to P-450p-2 from the cDNA library of human placenta. Gene structure and expression. Eur J Biochem 187:23–29.

Yu K, Bayona W, Kallen CB, Hardings HP, Ravera CP, McMahon G, Brown M, Lazar MA. 1995. Differential activation of peroxisome proliferator-activated receptors by eicosanoids. J Biol Chem 270:23975–23983.

Zheng YM, Fisher MB, Yokotani N, Fujii-Kuriyama Y, Rettie AE. 1998. Identification of a meander region proline residue critical for heme binding to cytochrome P450: Implications for the catalytic function of human CYP4B1. Biochem 37:12847–12851.